APPLYING HYPERSPECTRAL DATA TO INTERPRET VARIOUS CROP TYPES USING CHAOTIC EQUATIONS

I-Chen Yang, Re-Yang Lee, Chia-Hui Hsu
Department of Land Management, Feng-Chia University
No. 100, Wenhwa Rd., Seatwen, Taichung, 40724 Taiwan
e-mail:bird80224@hotmail.com

KEY WORDS: Chaos, Chaotic equation, Phenology, Hyperspectral

ABSTRACT: Chaos can be explained as nonlinear systems exhibit irregular movement patterns under certain circumstances. In other words, the systems appear to be irregular, but actually exhibit a certain degree of regularity in the irregularity. Crops grow continuously with fixed growth cycles, and the spectral reflectance value of crops is affected by the growth conditions (e.g., moisture, nutrition, and disease and pest damages), soil, and differences in natural phenomena such as solar irradiation and atmospheric conditions. These differences can cause slight deviation and irregularity in crop spectral reflectance curves. However, as phenology presenting a certain regularity, is quite accord with chaos. The current classification methods are applicable for specific crops and at specific locations and times. However, these methods lack generalizability. Thus, in nonlinear systems under certain conditions, the feasibility of applying chaos theory to remote-sensing crop classification is worthy of exploration. Therefore, this research utilizes the spectral reflectance values of various crops to interpret different crop types by employing chaos theory. The chaotic equation and the hyperspectral data collected by the handheld spectra-radiometer are used to create chaotic graphs. These graphs are then applied to differentiate different crop types. The MATLAB software is used to develop the models.
Three types of crop hyperspectral data sets, including garlic, scallion and sweet potato, are collected from the fields in Yunlin County, Taiwan. The results show that hyperspectral data sets derived from the crops can produce chaotic graphs using the chaotic equations. Since the spectral curves of crops are continues and highly sensitive to small changes, chaos theory can be applied to classify various crop types using hyperspectral data sets.

1. INTRODUCTION

Chaos theory is a method used in both qualitative and quantitative analysis for exploring the behavior of dynamic systems that can only be predicted using overall and continuous data relationships instead of single data relationships. Thus, chaos theory is suitable for predicting crop phenology. The theory has been applied in numerous domains such as natural systems, climate models, fluid movements, migration trends, communication systems, business management (Trygestad, 1997), ecology (Kauffman, 1991), and economics (Kelsey, 1988). However, no study has applied chaos theory to remote sensing.

In the past, scientists investigated the chaos phenomenon in electronic circuit systems as a precursor to investigating chaos in real systems. The chaos phenomenon was originally calculated using mathematical algorithms in computers to predict climate change. Circuit systems exhibit high fitness to corresponding mathematical models, thereby facilitating simulating various circuit systems and repeating various complex nonlinear phenomena. Thus, exploring the chaos phenomenon from the perspective of electronic circuit systems is appropriate. Chua's circuit has been extensively employed in practical operations. Because it is a typical nonlinear chaotic circuit with a simple structure that can be easily performed in engineering experiments, chaos phenomena can be generated within appropriate parameter ranges. Thus, Chua's circuit was selected in the present study as a foundation for remote-sensing applications.

Because of its characteristics of a wide data coverage area, low cost, repeated observation and monitoring, high time efficiency, and the absence of terrain or traffic restrictions, remote-sensing technologies have become crucial survey tools that are gradually replacing conventional time-consuming and laborious ground survey tools. In agricultural management, satellite remote-sensing images have been employed in surveying crop cultivation areas (Gallego, 2004; Pittman et al., 2010; Wan et al., 2010), monitoring crop growth (Doraiswamy et al., 2004; Busetto et al., 2008), predicting crop yield (Doraiswamy et al., 2003; Chang et al., 2005; Wang et al., 2010; Becker-Reshef et al., 2010), identifying spectral difference between tree species (Lawrence et al., 2006; Clark & Roberts, 2012; Dalponte et al., 2012; Naidoo et al., 2012), and analyzing area damage and the extent of loss from natural disasters (Qin et al., 2008; Becker-Reshef et al., 2010).

Previous studies have adopted various methods and applications with specific advantages and applicability. However, crops grow continuously with fixed growth cycles, and the spectral reflectance value of crops is affected by the growth conditions (e.g., moisture, nutrition, and disease and pest damages), soil, and differences in natural phenomena such as solar irradiation and atmospheric conditions. These differences can cause slight deviation and irregularity in crop spectral reflectance curves. The aforementioned classification methods are applicable for specific crops and at specific locations and times. However, these methods lack generalizability. Thus, in nonlinear systems under certain conditions, the feasibility of applying chaos theory to remote-sensing crop classification is worthy of exploration.

A chaotic algorithm requires entry of a series of data. Obtaining continuous data from current commercial satellites or aerial images is difficult because of climate conditions and budget constraints. However, hyperspectral ground images captured by portable devices exhibit numerous wavebands and narrow spectral ranges. Spectral ranges that are similar form continuous data. Spectral information in hyperspectral images is richer than that in ordinary multispectral images, rendering them useful for detecting minor spectral differences. Such differences overcome the insufficiency in multispectral images. Portable spectroradiometers can be used to measure the on-site reflectance curves of various land features at various times, locations, and statuses. Because crops change continuously and rapidly according to temporospatial conditions (e.g., etiolation, abscission, disease, unevenly distributed spatial density, and differences in planting times), a considerable number of variables are added to crop

spectra, which is the primary cause of difficulty in classifying crops. Chaotic algorithms may be suitable for solving the crop classification problem and effectively identify various crop categories.

In conventional image interpretation, scallion and garlic are easily confused, which can lead to misjudging the planting area and yield of both crops. Because these two crops are essential economic crops in Taiwan, distinguishing them is necessary. Thus, hyperspectral data of scallion and garlic plantations were employed to examine whether continuous spectral data combined with Chua's circuit chaotic equation can distinguish scallion and garlic plantations. Chua's circuit is composed of five linear elements and one nonlinear element (Cruz and Chua, 1992; Chua, 2007). When continuous spectral data of different crops are inputted into the model, chaos behaviors occur. Analyzing the resulting chaos images was expected to enable identifying various crop categories correctly, thereby achieving the goal of crop classification. According to the characteristics of the overall prediction results, which were influenced by slight deviations in the input data, chaos theory should be suitable for application in remote-sensing technologies for distinguishing crop categories. The research sample investigated in the present study comprised garlic, scallion, sweet potato, and carrots, most of which are planted in Yunlin County and are easy to sample. The chaotic image features of spectral reflectance of the various crops were captured at the same time and compared to discern any differences. MATLAB was used to develop the Chua's circuit chaotic equation before conducting the chaos simulation.

2. MATERIALS AND METHOD

2.1 Study Area

The sampling location was in the western region of Yunlin County, including Taixi Township and a part of Dongshi Township (Fig. 1). Yunlin County is a crucial crop production region of Taiwan, yielding the highest agricultural production among all counties in Taiwan. Because Yunlin County is located in a subtropical climate zone, the average annual temperature is 22.6 ℃ and the average annual precipitation is 1,028.9 mm.

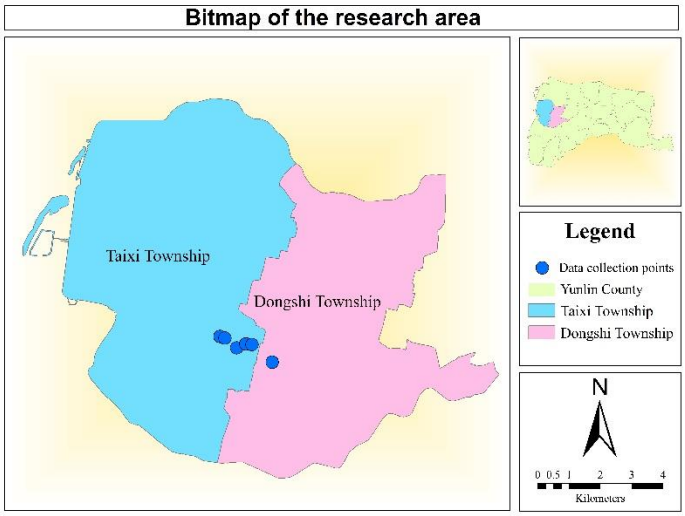

Figure 1. The research area

2.2 Collection of Crop's Hyperspectral Reflectance Data

2.2.1 Instruments and procedures of the field work

Crop spectral data (spectral reflectance) in the present study were obtained using PSR-1100 field portable spectroradiometers. The spectral range was 320–1050 nm and the spectral sampling interval was 1.5 nm. The actual number of measured wavebands was 512 and the angle of view was 4°. Other measurement instruments include a personal digital assistant (PDA), correcting whiteboard, thermometer and hygrometer, and tape measure. The spectroradiometer was mounted on a tripod during the field survey. The properties measured during the field survey included the brightness, luminance reflectance, spectral reflectance, and spectral distribution.

The measurement of reflectance was completed within 2 hours at approximately noon. During sample collection, it was necessary to minimize the interference from manual operation factors. Thus, the measurers wore dark clothes to reduce the errors. When the spectroradiometer was mounted on the tripod, it was placed above the crops and adjusted to avoid the effect of shade from the instrument. Subsequently, the measurer maintained a distance from the spectroradiometer and collected spectral data via a Bluetooth connection between the PDA and spectroradiometer. To reduce the errors resulting from sudden changes in solar radiation, a whiteboard specifically for detecting reflectance was used to correct for solar radiation to avoid inaccurate spectral reflectance caused by sudden changes in the ambient light field intensity.

2.2.2 Field samples collection

From November 2013 to February 2014, the researchers captured the spectral reflectance of samples at the research area on nine occasions with 7–10-day intervals. The intervals differed because of climate factors, such as samples cannot be measured when it rained. The sample was garlic, which was easy to sample because it is the dominant crop in Yunlin County. The growth period of garlic is between October and March. Although the planting time of garlic differs annually, the primary objective of the present study was to determine the dates when crops can be discerned clearly. To prevent the garlic being planted on different dates from influencing the analysis results, the date when the garlic was planted in the study plantation (October 1) was used as the baseline date for the analysis. Scallion, sweet potato, and carrot, which are common in the study area and easily confused with garlic, were also added as targets. The total sample observations of scallions, garlic, sweet potatoes, and carrots were 27, 27, 9, and 9.

Before spectral data were collected in the field, a whiteboard was used to simulate the 100% reflectance and prevent changes in the solar incident angles from influencing the results. Thus, after the direct energy (DE) of the plants was captured, the whiteboard correction values recommended by the manufacturer of the spectroradiometer were applied for waveband correction. Finally, the DE values were converted to reflectance values.

2.3 Execute Chua's circuit chaotic equation in MATLAB

The objective of the current study was to establish a chaotic pattern that could represent the target crops. Spectral series was used for the analysis. In other words, the 512 wavebands of one crop at specific time points were substituted into the chaotic equation during each calculation. The Chua circuit chaotic equation developed using MATLAB was used for the simulation. The crop spectral reflectance values were inputted into the equation to generate chaotic patterns of each crop for interpretation.

The chaotic equation generated chaotic patterns through moderators. The following three conditions must be met to generate a chaotic pattern: (1) at least one nonlinear parameter (element), (2) at least one resistor dissipating energy, and (3) at least three energy storage parameters (elements). Thus, Chua's circuit equation comprises four linear elements: capacitances C_1 and, C_2; inductance *L*, resistance *G* = 1 / *R*, and the nonlinear element of Chua's diode nonlinear resistance N_r. Fig. 2 shows Chua's circuit equation.

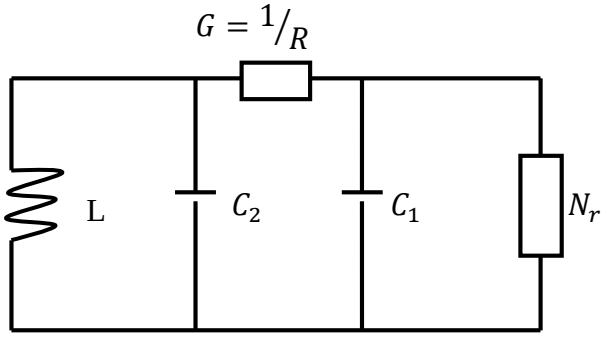

Figure 2. Chua's circuit

Chua's circuit equation is a first-order differential equation:

$$\begin{cases} \frac{dI_3}{dt} = -\frac{1}{L}V_2 \\ \frac{dv_2}{dt} = \frac{1}{C_2}I_3 - \frac{G}{C_2}(V_2 - V_1) \\ \frac{dv_1}{dt} = \frac{G}{C_1}(V_2 - V_1) - \frac{1}{C_1}f(V_1) \end{cases} \quad (1)$$

where V_1 and V_2 denote the voltages of the two ends of C_1 and C_2, respectively, and the current flowing through inductance L is I_3. The voltages and current compose a 3D nonlinear element. The 3D trail (I_3(t), V_2(t), V_1(t)) depicts the changes in chaos status. The 2D trail (V_1(t), V_2(t)) is called a phase space, in which $f(V_1)$ is the voltage–current (*V*–*I*) characteristic curve describing Chua's diode nonlinear resistance N_r (Fig. 3). The polynomial is expressed as follows:

$$f(V_1) = G_b V_t + \frac{1}{2}(G_a - G_b) \times [|V_1 + E| - |V_1 - E|]. \quad (2)$$

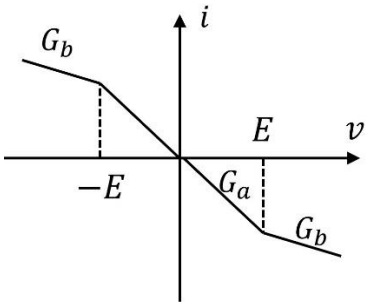

Figure 3. V–I characteristic curve of the nonlinear resistance N_r

The terms G_a and G_b in the polynomial respectively represents the characteristic internal curve slope and external curve slope. E represents the breakover voltage.

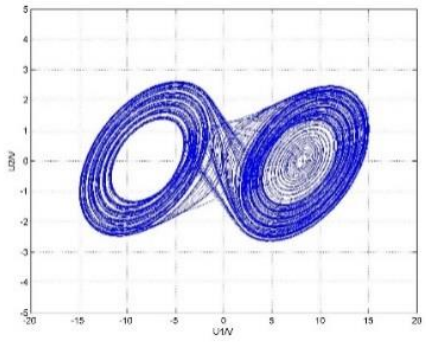

Figure 4. Chaotic pattern involving dual attractors

The spectral data were substituted into the Chua's circuit chaotic equation. The 2D phase space (V_1(t), V_2(t)) was obtained (Fig. 4), in which the X axis represents the voltage at both ends of C_1, and the Y axis represents the voltage at both ends of C_2. A chaotic pattern with dual attractors was generated according to the phase space. After the chaotic patterns were constructed, the differences between the patterns were analyzed. The critical values of each pattern in the 2D spaces were used in an inductive analysis and exploration.

2.4 Spectrum series analysis

Wavebands (320–1050 nm with an interval of 1.5 nm; 512 measurements) were simulated in a temporal axis. The reflectance of each waveband corrected using the whiteboard represented the strength of the input voltage V_2, which was substituted into Chua's circuit chaotic equation for the simulation. Subsequently, an analysis was conducted on the chaotic patterns with the attractors derived from the equation. The chaotic patterns generated the 2D phase spaces by using V_1(t) and V_2(t). The maximum and minimum values of the chaotic patterns were summarized to define the chaos range of each crop. The difference between the chaotic patterns was employed to distinguish the crops and establish a pattern database for them. The sampled crops comprised scallions, garlic, sweet potatoes, and carrots. Scallion and garlic samples were collected from three locations at nine time points. Thus, data from 27 sample observations were collected for both crops. However, because the sweet potato

and carrot data were sampled at one location, only nine sample observations were collected for both crops.

3. RESULTS AND DISCUSSIONS

In the spectral series analysis, the 512 spectral reflectance values obtained for each crop were substituted into Chua's circuit chaotic equation. The chaotic pattern of each crop exhibited continuous oscillation results of $V_1(t)$ and $V_2(t)$ for 1 ms. Figures 5 depict the 2D phase spaces of garlic. To facilitate an analysis, the three maximum and minimum values of the garlic reflectance generated from the $V_1(t)$ and $V_2(t)$ oscillation critical values were averaged, and the scallion reflectance underwent an identical averaging process. Because the minimum values of the crops exhibited only a slight difference, only the maximum values of $V_1(t)$ and $V_2(t)$ of the crops (Table 1) were used in the subsequent analysis.

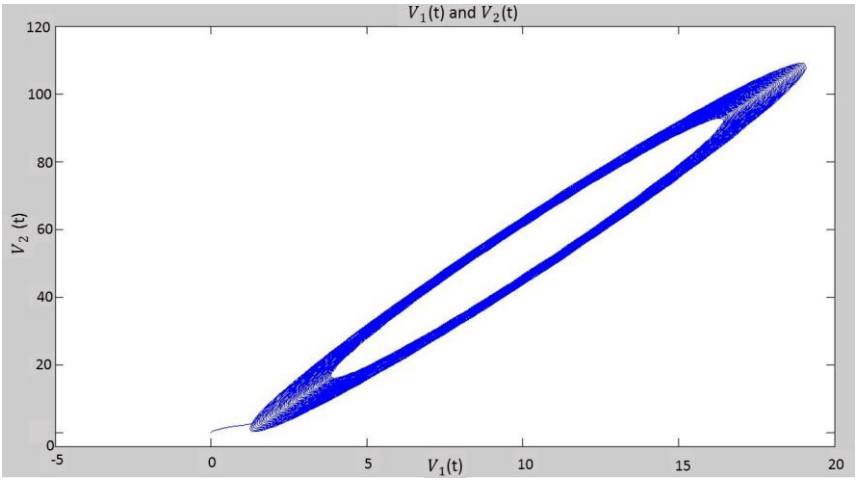

Figure 5. Garlic 2D phase space on December 20 (81)

Table 1 Maximum values of $V_1(t)$ and $V_2(t)$ of crop chaotic patterns

		11/12 (43)*	11/26 (57)	12/06 (67)	12/20 (81)	12/24 (85)	01/07 (99)	01/16 (108)	01/28 (120)	02/21 (144)
scallion	V_1（t）	2.560	2.877	2.617	2.527	2.831	2.586	2.840	2.684	3.758
	V_2（t）	9.001	10.900	9.388	8.791	10.666	9.160	10.680	9.759	16.240
garlic	V_1（t）	3.618	2.264	3.236	2.838	3.310	4.074	3.860	3.567	3.775
	V_2（t）	15.365	7.210	13.068	10.684	13.540	18.147	16.855	15.120	16.346
sweet potato	V_1（t）	4.119	4.108	2.953	3.255	2.983	3.731	3.387	3.211	2.042
	V_2（t）	18.459	18.393	11.353	13.155	11.531	16.030	14.008	12.920	5.885
carrot	V_1（t）	3.766	3.894	2.465	3.671	2.637	3.390	3.243	3.501	2.216
	V_2（t）	16.235	17.055	8.444	15.709	9.440	14.080	13.179	14.679	6.926

*Values inside the parentheses indicate the number of days for growing garlic; October 1 is the baseline.

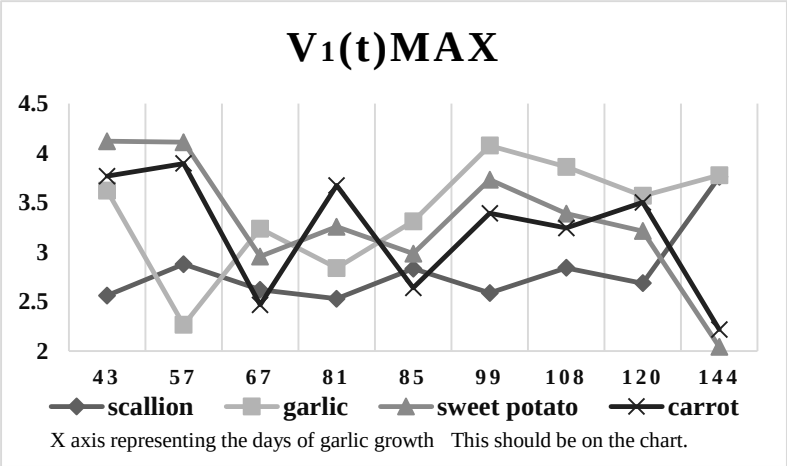

Figure 6. V_1(t) Changes in maximum values of chaotic patterns of the crops in different periods.

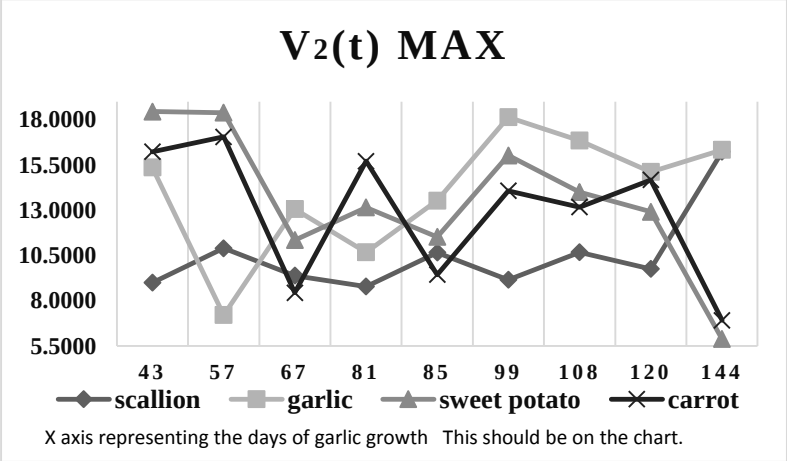

Figure 7. V_2(t) Changes in maximum values of chaotic patterns of the crops in different periods.

Figures 6 and 7 depict the V_1(t) and V_2(t) maximum values of the crops in each period. The trends in the two figures are identical. According to the nine data observation time points, the garlic is clearly distinguishable from other three crops except on Days 43 and 120. On Days 67, 85, and 144, scallion was easily confused with the other crops. On Days 81 and 99, all four crops were clearly distinguishable. However, because the sweet potato and carrot data were collected at only one location, the representativeness is low. These data can serve only as a comparison reference for the present study.

4. CONCLUSIONS AND SUGGESTIONS

4.1 Conclusions

A chaotic equation was used in a ground-based hyperspectral analysis. Spectral data of the crops were input into a model to generate chaotic behavior. Through nonlinear concepts, various crop models were established. According to previous studies, hyperspectral crop data substituted into a chaotic equation can generate chaotic behavior because crop spectra possess consistently high sensitivity to slight differences and features continuity. Thus, chaos theory can be applied to hyperspectral image-based crop classification.

In spectral series analysis, the spectral reflectance characteristics of chaotic patterns of different crops captured at the same time were compared. Among the nine sample observation time points, suitable time points for discerning the crops were assessed and recommended for capturing crop reflectance in the future. The results revealed that on Days 81 and 99, the four crops were clearly distinguishable. In other words, if garlic was planted on October 1, then December 20 and the following January 7 would be effective time points for distinguishing garlic, scallion, sweet potato, and carrot by using spectral data.

Chaos theory has been applied in studies in electrical and information engineering, medicine, fluid dynamics, neural network, ecology, and physical chemistry. However, to date, no study has applied it in the remote-sensing domain; thus, the present study is a pioneer study that can serve as a reference for practical agricultural management.

4.2 Suggestions

Because chaos theory was applied in remote sensing for the first time, much improvement can be achieved in the future. According to the problems encountered in the research process, the following suggestions are provided for future studies.

First, measuring chaotic patterns is problematic. The 2D phase space of V_1(t) and V_2(t) was employed to determine the maximum values of the chaotic pattern results and explain the differences among the crops. The complex patterns represented by a single value over-simplified the explained minute changes in the chaotic patterns. Future studies can adopt fractal dimensions to measure chaotic patterns more accurately, thereby increasing the discriminatory power of crop spectral reflectance.

Second, only a few crop reflectance locations were selected in this study (three for garlic and scallions and one for sweet potatoes and carrots). Consequently, the representativeness was too low to explain the differences among the crops. Therefore, future studies should acquire more location data for each crop to establish a reliable spectral reflectance models. In addition to discerning various known crops, the models should be able to interpret unknown crops.

Finally, an analysis of the 512 collected wavebands resulted in excess data and information interference. Future studies should analyze the time series of each waveband to identify the specific wavebands that exhibit the most favorable discriminatory power. Subsequently, chaotic patterns created from these specific wavebands should be sufficient to establish an optimal classification model.

5. References

Busetto, L., Meroni M., and Colombo, R., 2008. Combining medium and coarse spatial resolution satellite data to improve the estimation of sub-pixel NDVI time series. Remote Sens. Environ, 112: 118-131.

Chang, K.W., Y. Shen, and J.C. Lo., 2005. Predicting rice yield using canopy reflectance measured at booting stage. Agron. J. 97:872-878.

Clark, M. L. and Roberts D.A., 2012. Species-level differences in hyperspectral metrics among tropical

rainforest trees as determined by a tree-based classifier. Remote Sens. 4:1820–1855.

Cruz and Chua, L. O., 1992. A CMOS IC Nonlinear Resistor for Chua`s Circuit ", IEEE CAS, 39, 985-995,.

Dalponte, M., L. Bruzzone and Gianelle D., 2012. Tree species classification in the Southern Alps based on the fusion of very high geometrical resolution multispectral/hyperspectral images and LiDAR data. Remote Sens. Environ. 123:258–270.

Doraiswamy, P.C., Hatfield J.L., Jackson T.J., Akhmedov B., Prueger J., Stern A., 2004. Crop condition and yield simulations using Landsat and MODIS. Remote Sens. Environ, 92: 548-559.

Doraiswamy, P.C., S. Moulin, P.W. Cook, Stern A., 2003. Crop yield assessment from remote sensing. Photogramm. Eng. Remote Sens, 69: 665-674.

Gallego, F. J., 2004. Remote sensing and land cover area estimation. Int. J. Remote Sens, 25: 3019-3047.

Guess, D. & Sailor W., 1993. Chaos theory and the study of human behavior: Implications for special education and developmental disabilities. Journal of Special Education, 27(1), 19-34.

Kauffman, S. A., 1991. Antichaos and adaptation. Scientific American, 265: 78-84.

Kelsey, D., 1988. The economics of chaos of the chaos of economics. Oxford Economic Papers, 40: 1-31.

Leon O. Chua., 2007, Scholarpedia, 2(10):1488. " Chua Circuit " Curator: Dr. Leon O. Chua, Dept. of EECS, University of California, Berkeley. J. M.

Naidoo, L., M.A. Cho, R. Mathieu and Asner G., 2012. Classification of savanna tree species, in the Greater Kruger National Park region, by integrating hyperspectral and LiDAR data in a Random Forest data mining environment. ISPRS J. Photogramm.. 69:167–179.

Pittman, K., Hansen M.C., Becker-Reshef I., Potapov P.V., Justice C.O., 2010. Estimating global cropland extent with multi-year MODIS data. Remote Sens, 2: 1844-1863.

Qin, Q., A. Ghulam, L. Zhu, L. Wang, J. Li, Nan P., 2008. Evaluation of MODIS derived perpendicular drought index for estimation of surface dryness over northwestern China. Int. J. Remote Sens, 29: 1983-1995.

Strunk, V. L., 1995. A study of transition boundaries in organizational evolution: The punctuated equilibriummodel. Wal-den University, Unpublished Dissertation. AAC95336779

Trygestad, J., 1997. Chaos in the classroom: An Application of chaos theory. Paper presented at the Annual Meeting of the American Educational Research Association, Chicago, IL. ED413289

Wan, S., T.C. Lei, T.Y. Chou., 2010. An enhanced supervised spatial decision support system of image classification: consideration on the ancillary information of paddy rice area. International Journal of Geographical Information Science, 24: 623-642.

Wang, Y.P., Chang, K.W., Chen, R.K., Lo, J.C., and Shen, Y., 2010. Large area rice yield forecasting using satellite imageries. International Journal of Applied Earth Observation & Geoinformation 12: 27-35.